Earth-abundant elements a sustainable solution for electrocatalytic reduction of nitrate

Ana S Fajardo, Paul Westerhoff, Carlos M Sánchez-Sánchez, Sergi Garcia-Segura

Earth-abundant elements a sustainable solution for electrocatalytic reduction of nitrate

Ana S. Fajardo[a,b,*], Paul Westerhoff[a], Carlos M. Sanchez-Sanchez[b], and Sergi Garcia-Segura[a,**]

[a]Nanosystems Engineering Research Center for Nanotechnology-Enabled Water Treatment, School of Sustainable Engineering and the Built Environment, Arizona State University, Tempe, AZ 85287-3005, USA

[b]Sorbonne Université, CNRS, Laboratoire Interfaces et Systèmes Electrochimiques (LISE), 4 place Jussieu, F-75005, Paris, France

Corresponding author:

*e-mail: adossan3@asu.edu (Dr. Ana Sofia Fajardo)

**e-mail: Sergio.garcia.segura@asu.edu (Dr. Sergi Garcia-Segura)

Abstract

Platinum group elements (PGEs) are widely-used electrocatalysts. However, the low abundance of PGEs in the earth's crust and high environmental impacts to be acquired result in high costs, limiting their use in drinking water treatment. Identifying sustainable alternatives to PGEs is a major barrier in applying electrocatalysis for nitrate reduction. By moving up the periodic table, this study provides a framework for selecting promising earth-abundant elements that can electrocatalytically degrade nitrate in water to innocuous by-products. We benchmarked platinum (Pt) against less-endangered elements for electrodes by quantifying nitrate reduction rates, by-product selectivity, and energy efficiencies. Carbon (as boron-doped diamond) and tin had the highest average selectivity towards nitrogen gas evolution (55% and 64%, respectively) outperforming Pt, which only had 1% selectivity, and had comparable electrical energy per order removal of nitrate. Thus, earth-abundant elements for electrocatalysis hold tremendous promise as innovative, low-cost, and sustainable processes for the water treatment marketplace.

Keywords: water treatment; advanced reduction processes; electrochemical technologies; cathodic materials; selectivity towards nitrogen

1. Introduction

Ensuring access to safe water and sanitation is essential to health and a human right[1]. Nitrate pollution is one of the top ten most common water quality violations reported worldwide[2–5]. The World Health Organization (WHO) and United States Environmental Protection Agency set maximum concentration levels in drinking water of ~10 mg NO_3^--N L^{-1}.[6,7] Elevated NO_3^- levels in drinking water can cause cancer, thyroid problems, and adverse respiratory effects[8–11]. As a consequence of anthropogenic nitrogen fertilizer inputs, nitrate concentrations in surface and groundwater have dramatically increased during the last century[12]. There are ~45 million people in the United States that rely on unregulated private groundwater wells, many of which have nitrate above regulated limits[2,13]. In addition, many municipal water supplies are impacted by nitrate and are commonly treated using costly ion exchange technology[14–19]. Thus, there is a pressing need for efficient nitrate removal technologies suitable for large-scale water treatment systems as well as very small point-of-use (POU) treatment systems within homes[20,21]. In a comprehensive review, we recently summarized how electrocatalytic reduction of nitrate (ERN) can selectively reduce NO_3^- to innocuous dinitrogen (N_2) and serves as a viable drinking water treatment technology[22]. Because electrode cost dominates the capital cost of electrochemical systems, a thorough revision on the state of the art with detailed description of the electrodes applied to (ERN) was performed as well[22–24]. The majority of publications on ERN utilized platinoid materials (i.e., Pt and Pd)[25–34]. Platinum electrodes are excellent electrocatalysts for nitrate reduction in the water-energy nexus due to its corrosion resistance [35–37]. Unfortunately, platinum group elements (PGEs) are labeled as expensive and endangered elements due to their high cost and limited availability as resources in our planet[38]. Lifecycle analysis pinpoints adverse environmental impacts related to extraction and purification of these endangered elements[39–42]. Scientific and engineering challenges lie on uncovering alternative electrocatalysts based in high-efficient earth-abundant elements.

Earth-abundant alternatives to PGE electrodes likely exist but have been barely explored. Analogues for electrocatalytic responses using non-endangered substitutes to PGE might be identified by moving up the periodic table. This research aimed to provide a framework for selecting promising earth-abundant elements to electrocatalytically degrade nitrate in drinking water. To the best of our knowledge, this is the first time a paper explored, under identical experimental conditions, a direct comparison of PGE-based electrodes against electrodes fabricated from earth-abundant elements of the first row transition metal d-block elements (e.g., Ti, Fe, Co, Ni, Cu, Zn) plus carbon (C) and tin (Sn). Operating conditions were selected to minimize side reactions with other electroactive species that may impact the fundamental understanding of the electrochemical transformations. Nitrate degradation rates, formation of aqueous intermediates (nitrite and ammonium ion), and selectivity towards gaseous by-products were quantified. Nitrogen gas is the preferred nitrate reduction by-product because (a) nitrite remains toxic to humans, (b) ammonia has odor and potential human health concerns, (c) ammonia reacts with chlorine disinfectants, and (d) nitrogen gases are permanently removed from solution. Engineering figures of merit were used to evaluate operational requirements for electrical energy per order (E_{EO}) and efficient use of electron delivered in terms of Faradaic efficiency. Results are discussed for relative cost and efficiency of earth-abundant elements as alternatives to Pt electrocatalysts.

2. Materials and methods

2.1 Electrochemical experiments

Electrochemical nitrate reduction was conducted using an open, undivided cylindrical glass batch reactor containing 200 mL of non-deaerated 100 mg NO_3^--N L^{-1} solutions with 50 mM Na_2SO_4 (pH = 5.86±0.07 and conductivity = 7.74±0.08 mS cm^{-1}) at 25 °C. Reagent grade sodium nitrate, sodium nitrite, and ammonia sulfate (>99%) were purchased from Sigma-Aldrich. Analytical-grade sodium sulfate (99%, Sigma-Aldrich) was used as the supporting electrolyte. All

87 solutions were prepared with ultrapure water with resistivity >18.2 MΩ cm at 25 °C (Millipore
88 Milli-Q system).

89 Batch reactor experiments were continuously mixed using magnetic stirring at 700 rpm to
90 reduce mass transport limitations between the bulk solution and the electrode surfaces. The
91 electrochemical cell was equipped with commercial sheet parallel electrodes of 2.5 cm × 2.4 cm
92 with a defined geometrical area of 6.0 cm^2 (area delimited with Teflon, back part and sides). The
93 interelectrode gap distance was 1.5 cm. A Ti/IrO_2 (DeNora) anode, and different cathodes were
94 tested: titanium (99.9%, McMaster-Carr), stainless steel (as iron element, Victor Monteiro), cobalt
95 (99.9%, Fine Metals), nickel (99.6%, Trudsafe), copper (99.9%, CynKen), zinc (99.9%, Filzinc),
96 carbon cloth (99.5% carbon content, Fuel Cell Store), carbon felt (99.0% carbon content, Fuel Cell
97 Store), synthetic boron-doped diamond (BDD; Adamant Technologies), tin (99.9%, McMaster-
98 Carr), and a polycrystalline platinum (99.9 %, Stanford Advanced Materials). The electrocatalysts
99 were rinsed with ultrapure water before use. The carbon-based materials (see specifications in
100 Supplementary Information (SI) Table S1) were activated in a solution containing 50 mM of
101 Na_2SO_4 at 100 mA cm^{-2} for 120 min.

102 Experiments were conducted galvanostatically using a TENMA 72-13610 DC power
103 supply under constant applied current density of 20 mA cm^{-2}. To evaluate the possible re-oxidation
104 of reduction by-products to nitrate, control experiments with Sn were performed using initial
105 solutions of 100 mg L^{-1} NO_2^--N or 100 mg L^{-1} NH_3-N solutions with 50 mM Na_2SO_4, the details are
106 shown in SI, Figure S1a and S1b, respectively. It was detected that a slight oxidation of nitrite to
107 nitrate may occur on the surface of the anode. However, that re-oxidation did not seem meaningful
108 when compared to nitrite's reduction to nitrogen gas (Figure S1a). No ammonia oxidation was
109 observed (Figure S1b). Because the oxidation reactions occur at the anode and the electrode
110 material was always the same, only one control was needed. Samples were collected over time and
111 analyzed for aqueous nitrogen species, conductivity, and pH. Experiments were run in triplicate,
112 and deviations between them were lower than 5% for all trials.

2.3 Analytical techniques

The pH and conductivity were measured over time using a 2 Hanna Instruments HI 322 and VWR Scientific Products - EC Model 2052 meters, respectively. Nitrate and nitrite were quantified using ionic chromatography. Sample aliquots of 20 μL were injected in Thermo Dionex ICS-5000DC equipment coupled to a conductivity detector AERS 500, fitted with a high capacity hydroxide-selective anion-exchange column Dionex Ionpac AS18 (2 mm × 250 mm) column at 30 °C. A 10–45 mM KOH gradient solution at 0.25 mL min^{-1} was used as mobile phase per EPA 300 method[43]. Aqueous ammonia was measured according to Hach Method 10205, a salicylate-based ammonia chemistry that is equivalent to EPA 350.1, EPA 351.1, and EPA 351.2. Measurements used HACH DR6000 UV-vis equipment at 694 nm applying TNT 830 HACH kits. Reproducible NO_3^--N, NO_2^--N, and NH_3-N concentrations were obtained with an accuracy of 1%. Nitrate removal (NR) was calculated using Eq. (1)[44].

$$NR(\%) = \frac{C_{nitrate,i} - C_{nitrate,t}}{C_{nitrate,i}} \times 100 \quad (1)$$

where $C_{nitrate,i}$ is the nitrate concentration in mg NO_3^--N L^{-1} at time zero, and $C_{nitrate,t}$ is the nitrate concentration at time (t).

Some publications quantified specific N-volatile species (N_2, NO, NO_2 or N_2O) that were generated during the electrocatalytic reduction of nitrate. However, most of the works report all the obtained gas was N_2. Therefore, in this work, the evolution of gaseous nitrogen species determined from mass balances on aqueous nitrogen species assumed noted as N-gas, but likely corresponds mostly to N_2. We do report ammonium ion concentrations, and near or above the pKa of 9.25 for NH_4^+/NH_3 some ammonia volatilization can occur but the Henry's constant is not very large and such losses from solution of ammonia gas would be highly depending upon mixing or gas-purging conditions. The selectivity (S_X) towards N-gas evolution and ammonia was calculated using Eq. (2)[45].

$$S_X(\%) = \frac{C_X}{C_{nitrate,i} - C_{nitrate,t}} \times 100 \quad (2)$$

where C_X represents the concentration (mg N L^{-1}) of a species, X, produced over time.

The NO_3^--N decay followed pseudo-first order reaction kinetics and was fitted (R^2>0.95) by a rate constant (k_1, s^{-1}). Because the electrode surface area (6 cm^2) was the same for all experiments, k_1 (s^{-1}) can be directly converted to a surface-normalized area (k_1/6 $s^{-1}cm^2$). Nitrate reduction was evaluated in terms of Faradaic efficiency (FE, Eq. (3)), which determines the number of electrons consumed in an electrochemical reaction relative to the expected theoretical conversion ruled by Faraday's law[22].

$$Fe(\%) = \frac{n\,F\,N_i}{3600\,I\,t} \times 100 \quad (3)$$

where n is the amount of electrons required per mol of product (mol), F is the Faraday constant (96 487 C mol^{-1}), N_i is the amount (mol) of product generated during the electrolysis, I is the applied electric current (A), t is the electrolysis time (h), and 3600 is a unit conversion factor (3600 s h^{-1}).

Electrical energy per order (E_{EO}), was used as an engineering figure of merit to benchmark the electric energy required to reduce NO_3^--N concentration by one order of magnitude in a unit volume calculated from Eq. (4) for batch operation mode[46].

$$E_{EO}(kWh\,m^{-3}order^{-1}) = \frac{E_{cell}It}{V_s log(C_0/C_t)} \quad (4)$$

where E_{cell} is the average of the cell potential (V), I is current intensity (A), t is time (h), V_s is solution volume (L), and C_0 and C_t are the initial and final concentration after one order of magnitude reduction.

Considering the relationship $\log(C_0/C_t) = 0.4343 \bullet t \bullet k_1$, the E_{EO} expression can be simplified assuming first-order kinetics according to Eq. (5) where 6.39×10^{-4} is a conversion factor:

$$E_{EO}(kWh\,m^{-3}order^{-1}) = \frac{6.39 \times 10^{-4} E_{cell} I}{V_s k_1} \quad (5)$$

3. Results and discussion

3.1 Platinum electrode performance as reference electrocatalyst for nitrate reduction

Electrochemical reduction of nitrate has been focused mostly on the study of platinum as standard cathodic material[47–49], therefore Pt is used herein to benchmark alternative electrodes based on more sustainable elements. Figure 1 shows nitrate reduction and evolution of nitrite intermediates as ammonium ion and nitrogen gas by-products. A pseudo-first order rate constant (k_1) fits well the observed nitrate degradation (k_1= 3.7×10^{-5} s^{-1}; R^2=0.996). The sluggish reduction kinetics on Pt is controlled by the first charge transfer reaction as limiting step (Eq. (6)). Bimetallic electrodes on PGEs are often required to reduce this barrier[50–54], but this was beyond the scope of this study. The initial reduction of nitrate towards nitrite follows a three-step electrochemical-chemical-electrochemical (ECE) mechanism described by Eqs. (6)-(8)[22].

$$NO_3^-{}_{(ad)} + e^- \rightarrow NO_3^{2-}{}_{(ad)} \qquad \textit{limiting step} \qquad (6)$$

$$NO_3^{2-}{}_{(ad)} + H_2O \rightarrow NO_2^{\bullet}{}_{(ad)} + 2OH^- \qquad (7)$$

$$NO_2^{\bullet}{}_{(ad)} + e^- \rightarrow NO_2^-{}_{(ad)} \qquad (8)$$

Nitrate reduction by-products kinetics did not show appreciable accumulation of NO_2^- intermediates; a maximum concentration of 2.2 mg NO_2^--N L^{-1} was reached at 120 min (Figure 1b). The observed trend occurs due to the high electrocatalytic activity of Pt reducing nitrite to nitrogen gas and/or ammonia following reactions (9) and (10), respectively [55,56]. The net reduction of nitrate presented takes into account that nitrite yielded may be re-oxidized at the anode in the undivided cell (see Fig. S1a). According to reactions (9) and (10), hydroxide ions (i.e., consumption of protons during nitrate reduction) are also generated, increasing the pH from 5.86±0.07 to 11.3±0.1 over time as shown in Figure 1a (dashed line). In this pH range, N_2 and NH_3/NH_4^+ are the thermodynamically most stable forms of nitrogen according to Frost-Ebsworth diagrams[22,57]. Note that ammonia volatilization was not observed in blank experiments. Fundamental electrochemical studies typically do not buffer pH, and effects of constant pH and other water

179 quality parameters (e.g., alkalinity, ion composition) could be evaluated in a second-tier framework
180 study. Note that during the reduction of nitrate higher amount of OH^- is yielded by electron (1.3
181 $OH^-/1e^-$ for nitrogen gas and 1.2 $OH^-/1e^-$ for ammonia) than H^+ produced in the anodic oxidation of
182 water (1 $H^+/1e^-$). Thus, the pH change observed also allows inferring that nitrate reduction takes
183 place.

$$NO_{2(ad)}^- + 2H_2O + 3e^- \rightarrow \frac{1}{2} N_{2(gas)} + 4OH^- \quad (9)$$

$$NO_{2(ad)}^- + 5\ H_2O + 6e^- \rightarrow NH_3 + 7OH^- \quad (10)$$

184

185 After 360 min of reaction, a 58% nitrate loss yielded 49.5 mg L^{-1} NH_3-N and 5.8 mg L^{-1} N_2-
186 N. The calculated selectivity towards nitrogen evolution ($S_{N_{gas}}$) was only 10% with preferential
187 production of ammonia (S_{NH_3}= 87%). The Pt selectivity is closely related to crystallographic
188 availability at the interface[58]. Fundamental studies using monocrystalline electrodes have
189 identified Pt(100) domains as essential for selective reduction towards N_2 following the Duca-Feliu-
190 Koper mechanism[59–61]. However, synthesis of monocrystalline Pt electrodes limits the electrode
191 size to a few millimeters. Introducing defects in crystalline structure affects selectivity of Pt
192 catalysts. Nitrogen evolution can be drastically reduced by the defects in symmetry as observed at
193 Pt [(1 0 0) x (1 1 0)] and [(1 0 0) x (1 1 1)] surfaces[62]. This is evident in commercial
194 polycrystalline Pt electrodes where all crystallographic facets are present in a random distribution
195 rather than a preferential orientation such as the one reported in single crystal Pt. This is the reason
196 for reduced selectivity towards nitrogen evolution observed in polycrystalline Pt electrodes, with
197 the characteristic behavior depicted in Figure 1.

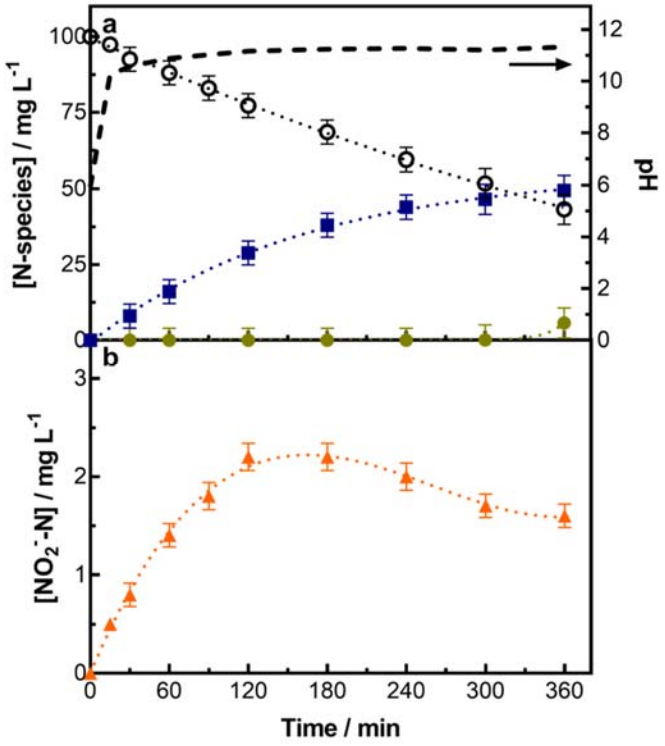

198

199 **Figure 1.** (a) Evolution of the nitrogenated species ((○) NO_3^--N, (■) NH_3-N, and (●) N_2-N) and
200 pH (long-dashed line) over time for the electroreduction of 100 mg L^{-1} NO_3^--N in 50 mM Na_2SO_4 at
201 20 mA cm^{-2}, using Pt as cathode material. (b) Evolution of nitrite ((▲) NO_2^--N) over time.

202

203 **3.2 Nitrate reduction kinetics of electrocatalysis materials upon moving up the periodic table**

204 Figure 2 shows the periodic table and identifies "endangered elements", which reflect their
205 relative earth abundance[38]. While platinum is considered a standard in electrocatalysis due to its
206 excellent properties, it is unfortunately an endangered element because of its limited abundance and
207 increasing use in products or processes[38]. The high electrocatalytic activity of Pt is associated
208 with the unclosed d-orbital shells of the metal, which contributes to the charge injection to the
209 lowest unoccupied molecular π* orbital of nitrate[22,63]. Transition metals resembling the electron
210 configuration of Pt are suitable for nitrate reduction but have not been the focus of comparative
211 studies. Thus, we compared the performance of transition metals for nitrate removal. By "moving

up the periodic table", catalysts using transition metals are more earth abundant and lower cost than Pt. The elements from the fourth period of the periodic table accomplish that requirement.

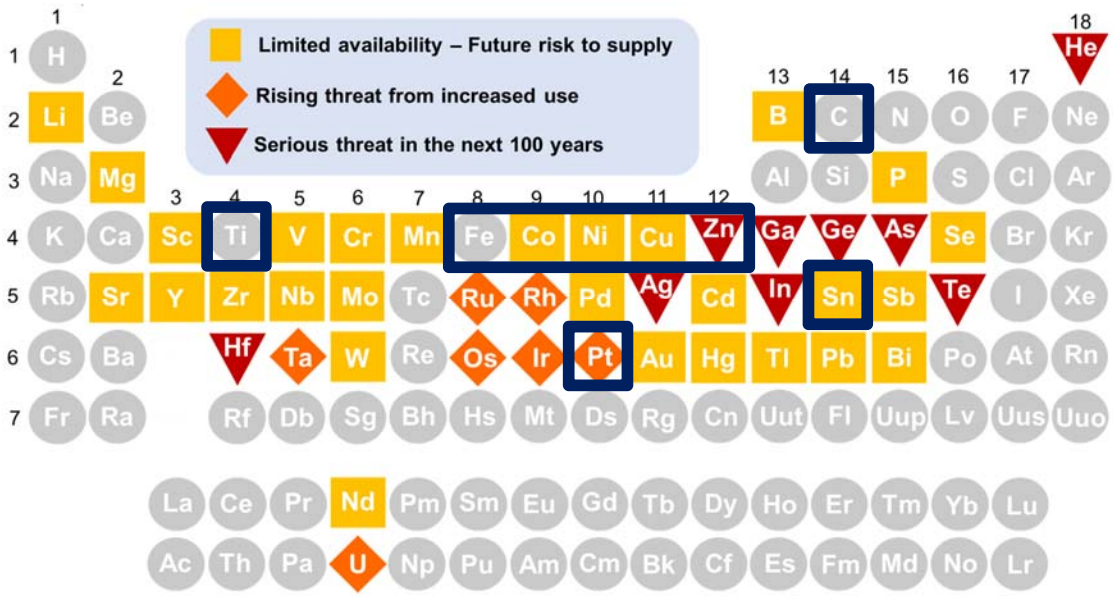

Figure 2. The periodic table's endangered elements (adapted from open source[38]). Elements availability: (●) high abundance, (■) limited availability, (◆) rising threat, (▼) serious threat in next 100 years.

Figure 3 depicts the performance of several transition metals materials to reduce nitrate under the same operating conditions. Fitted k_1 values fell within a narrow range (1.3 to 6.6×10^{-5} s^{-1}) (statistical fit details shown in SI, Figure S2). The low variability suggests a possible mass transfer rate limit that can be overcome through reactor engineering design.

Titanium (Ti) and iron (Fe) are widely available elements without a close depletion risk (Figure 2), but few direct comparisons of nitrate removal exist in the literature. Figures 3a and 3b illustrate that Ti (k_1 = 2.8×10^{-5} s^{-1}, R^2=0.993) and Fe (k_1 = 1.8×10^{-5} s^{-1}, R^2=0.997) electrodes both have ~2.0-fold slower nitrate reduction kinetics when compared with Pt. Table 1 summarizes key fitted and calculated parameters from all the experiments. For the Fe electrode, nitrite concentrations peaked at 2.7 mg L^{-1} NO_2^--N and followed trends similar to Pt. After 360 minutes of

229 reaction, the residual ammonium ion was 26 mg NH_3-N L^{-1}. $S_{N_{gas}}$ and S_{NH_3} using Fe were about
230 11% and 80%, respectively, also similar to Pt. For Ti electrode, nitrite accumulation peaked at 5.6
231 mg L^{-1} NO_2^--N at 180 min and decreased slowly to reach 4.5 mg L^{-1} NO_2^--N at 360 min. Consistent
232 with the literature[55,64–66], our Ti and Fe results showed ammonia generation was
233 electrocatalytically preferential over nitrogen gas evolution.

234 Cobalt (Co), nickel (Ni), and copper (Cu) are within the group of elements with limited
235 availability and possible future supply risk (Figure 2). Nitrate kinetics for these metals are shown in
236 Figures 3c, 3d, and 3e; Table 1 summarizes associated key parameters, and Figure S3 shows pH
237 evolution over time. Co had the highest nitrate reduction kinetics (~1.8-fold higher than Pt) and
238 produced the lowest nitrite (<0.08 mg NO_2^--N L^{-1}) throughout the experiment. Ni electrodes
239 achieved a high $S_{N_{gas}}$ (36%) but had amongst the slowest kinetics. Cu electrodes performed
240 between Ni and Co. Electrocatalytic reduction with Cu exhibited a slightly higher k_1 than Pt,
241 accumulated 3.8 mg NO_2^--N L^{-1}, and had $S_{N_{gas}}$ and S_{NH_3} of 28% and 64%, respectively. Cu
242 catalyzes the initial charge injection illustrated by Eq. (6), which is a rate limiting reaction for nitrite
243 formation. However, prolonged electrolysis preferentially reduces nitrite to ammonia instead of
244 nitrogen gas.

245 Zn electrodes had slightly higher k_1 than Pt (Table 1) and reached 60% nitrate reduction
246 after 360 min of treatment (Figure 3f). Zn showed the highest nitrite accumulation among the
247 evaluated elements in the fourth period of the periodic table, with maximum value of 17 mg NO_2^--N
248 L^{-1} at 240 min, decreasing during the following 120 min to 13 mg NO_2^--N L^{-1}.

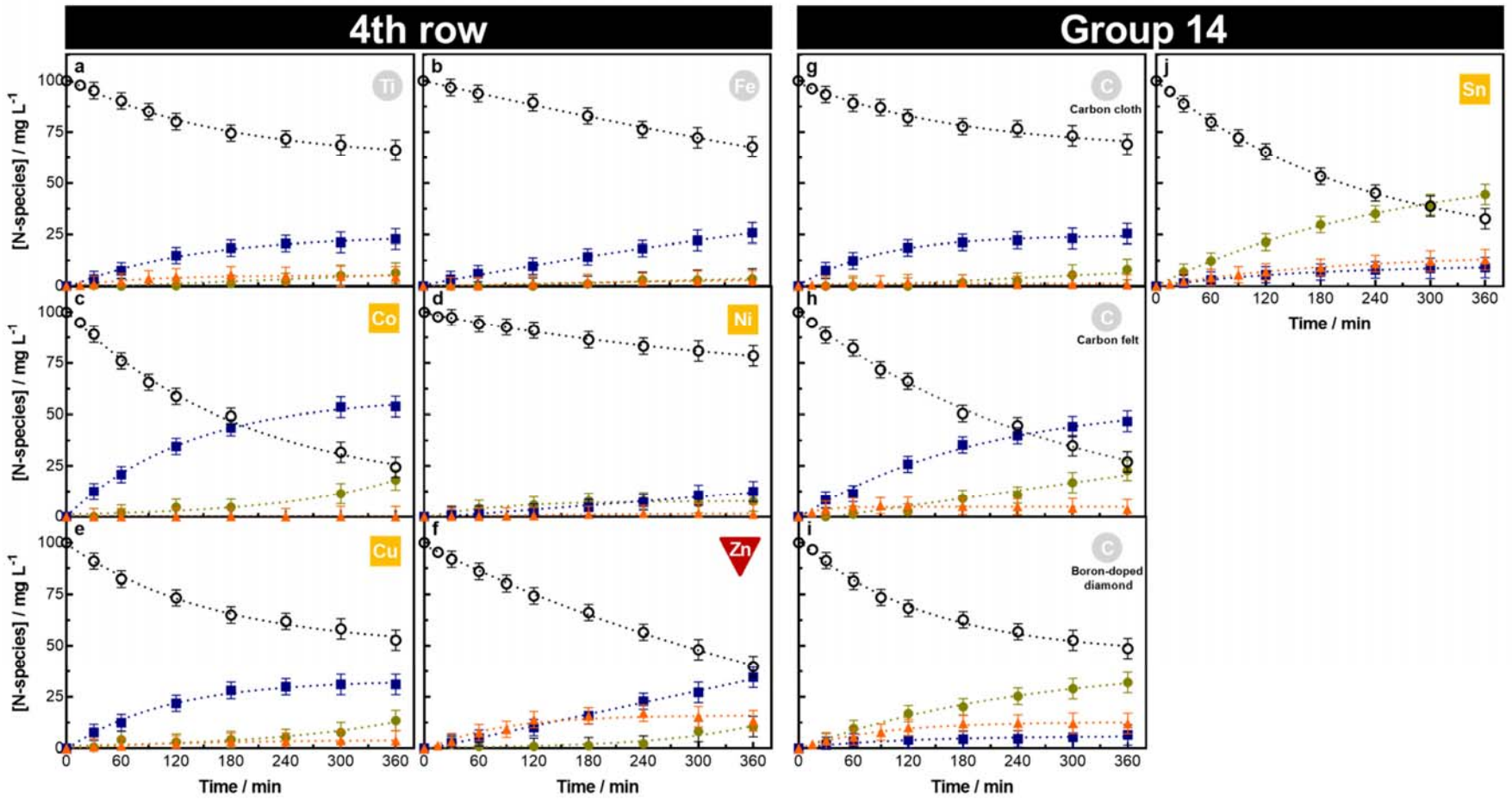

249

250 **Figure 3.** Evolution of the nitrogenated species ((○) NO_3^--N, (▲) NO_2^--N, (■) NH_3-N, and (●) N_2-N) over time for the electroreduction of 100 mg L^{-1} NO_3^--N in

251 50 mM Na_2SO_4 at 20 mA cm^{-2} using (a) Ti, (b) Fe, (c) Co, (d) Ni, (e) Cu, (f) Zn, (g) carbon cloth, (h) carbon felt, (i) boron-doped diamond, and (j) Sn.

252

253 **Table 1.** Key fitted and calculated parameters from all the experiments for the electroreduction of

254 100 mg L^{-1} NO_3^--N in 50 mM Na_2SO_4 at 20 mA cm^{-2} and 360 min of treatment time.

Electrode material	k_1, $\times 10^{-5}$ (s^{-1})	NR (%)	$S_{N_{gas}}$ (%)	S_{NH_3} (%)	Maximum (and t=360 min) nitrite (mg NO_2^--N L^{-1})
Pt	3.7±0.2	57±2	10±1	87±3	2.2±0.2 (1.6±0.3)
Ti	2.8±0.4	34±1	19±1	68±2	5.6±0.3 (4.5±0.5)
Fe	1.8±0.1	31±1	11±1	80±2	2.7±0.2 (2.7±0.2)
Co	6.6±0.5	76±3	25±2	75±1	0.08±0.01 (0.03±0.01)
Ni	1.3±0.2	21±1	36±1	58±1	1.6±0.3 (1.3±0.2)
Cu	4.2±0.3	47±2	28±2	64±3	3.8±0.4 (3.7±0.3)
Zn	4.1±0.3	60±1	18±1	59±2	17±2 (13±1)
Sn	5.4±0.4	67±3	67±3	14±1	13±1 (13±1)
Carbon					
Cloth	2.8±0.1	31±1	24±1	74±2	1.8±0.3 (0.7±0.1)
Felt	5.9±0.3	73±3	31±2	64±2	5.7±0.4 (3.6±0.3)
BDD	5.5±0.2	51±2	63±2	13±1	12±1 (12±1)

255

256 Tin (Sn) is not a 4th period d-block element in the periodic table, but it is widely reported as
257 an electrocatalyst[22]. Figure 3l shows that the tin electrode achieved 67% nitrate removal and
258 yielded the highest mass production of N-gases (44.5 mg N L^{-1}). Tin enhanced nitrate removal with
259 kinetics 1.5-fold higher than Pt and achieved the highest nitrogen gas concentration among the
260 electrode materials studied.

261 Each electrode material led to different trends for nitrate reduction and by-product
262 formation. The mechanism by which the material transfers electrons more easily to adsorbed nitrate
263 determines its suitability for pollutant removal. Nitrite is the first stable intermediate produced
264 during nitrate reduction. The further electrochemical reduction of this species can yield ammonia
265 (reaction (10)) and innocuous nitrogen gas (reaction (9)). Nitrite and ammonia are harmful to
266 human health and cause operational problems in drinking water systems, therefore making them
267 undesired by-products from nitrate reduction[22].

3.2.2. Carbon-based materials

Carbon is one of the most abundant elements on Earth[38]. Carbon-based materials have a diversity of structures, good electrical, thermal conductivity, and high mechanical strength, making carbon stand out as an electrode material[67]. Carbonaceous electrodes, such as carbon cloth and carbon felt, can be 1000-fold cheaper than PGEs. Carbon cloth and felt (Figures 3g and 3h) yielded a 1.8-fold lower k_1 than Pt (Table 1). Nitrite concentrations with carbon cloth reached a maximum of 1.8 mg L^{-1} NO_2^--N at 120 min and decreased to 0.73 mg L^{-1} NO_2^--N at 360 min. Overall, carbon felt performed better (higher $k_1$values) than Pt, carbon cloth, and most of the transition metals. One factor that may explain the superior performance of carbon felt is that its high porosity and large pores formed by interlace fibers allow the electrolyte to flow through the felts, favoring the reactants transport and reducing the cell resistance[68–70].

BDD electrodes achieved the most favorable outcomes among the carbon-based electrodes. Most notably, BDD achieved the highest selectivity towards desired gaseous N by-products ($S_{N_{gas}}$=63%) while also degrading nitrate 1.5-fold faster than the Pt electrodes (Figure 3i and Table 1). Due to its high stability under aggressive high acidic/alkaline media[71], corrosion resistance, low electrocatalytic inhibition[72], and belonging to the group of elements most available, BDD is a promising electrode for the electrocatalytic reduction of nitrate (ERN).

3.3. Benchmarking electrocatalysts towards higher electrokinetics and selectivity

Electrochemical reduction applicability is defined by treatment kinetics and selectivity (i.e., preferential formation of N_2). Technology competitiveness in market settings will be defined by techno-economic aspects related to material cost and availability, which goes beyond treatment performance. While market costs are good indicators of electrode costs for some elements (e.g., Pt) (see Fig. S4), the actual capital costs for low-cost elements may be further influenced by electrode synthesis processes and net manufacturing costs. For example, the three carbon-based electrodes

demonstrated that even for a single earth-abundant element (i.e., carbon), the electrode morphology, element oxidation state, and element bonding configuration played a major factor in overall electrode performance. Manipulating the element's morphological and chemical properties influence the synthesis or manufacturing costs of electrodes. This is true for most of the elements studied herein. For example, while elemental Ti plate was used here, other researchers observed that Magneli phase of titanium oxide (e.g., Ti_4O_7) can also degrade nitrate[73]. The numerous oxidation states of many of the earth-abundant elements, compared with the almost exclusive reliance on elemental metals in application of PGE electrodes, offer a remarkable "design space" for use of non-endangered elements as electrode materials.

Figure 4 benchmarks each electrocatalyst against Pt (◆) in terms of kinetics and selectivity obtained at 20% of nitrate removal, while considering sustainability aspects of different elements. Note that several electrocatalysts (Co, Cu, Zn, carbon felt, BDD, and Sn) outperformed Pt for NO_3^- reduction kinetics, which is illustrated by their location in the upper half of Figure 4b.

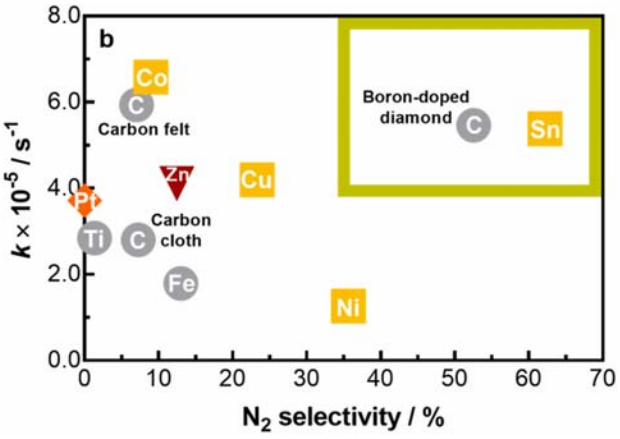

Figure 4. Pseudo-first order kinetics obtained vs. selectivity towards N_2 during electrochemical reduction of 100 mg L^{-1} NO_3^--N in 50 mM Na_2SO_4 at 20 mA cm^{-2} (values set at 20% of initial NO_3^- abatement). The electrocatalysts included in the upper right quadrant present the fastest reduction kinetics and highest selectivity towards nitrogen gas. Elements earth availability color coded based upon Figure 2: (●) high abundance, (■) limited availability, (◆) rising threat, (▼) serious threat in next 100 years.

For water treatment, the viability of electrodes fabricated from different elements depends strongly on by-product selectivity towards innocuous nitrogen gas rather than selectivity toward nitrite or ammonia. In Figure 5a, the average of selectivity towards nitrogen is plotted with error bars showing that this parameter varies minimally across the duration of the electrochemical treatment for most of the elements studied. In fact, this behavior can be verified in Figure 5b, with BDD and Sn attaining the highest $S_{N_{gas}}$.

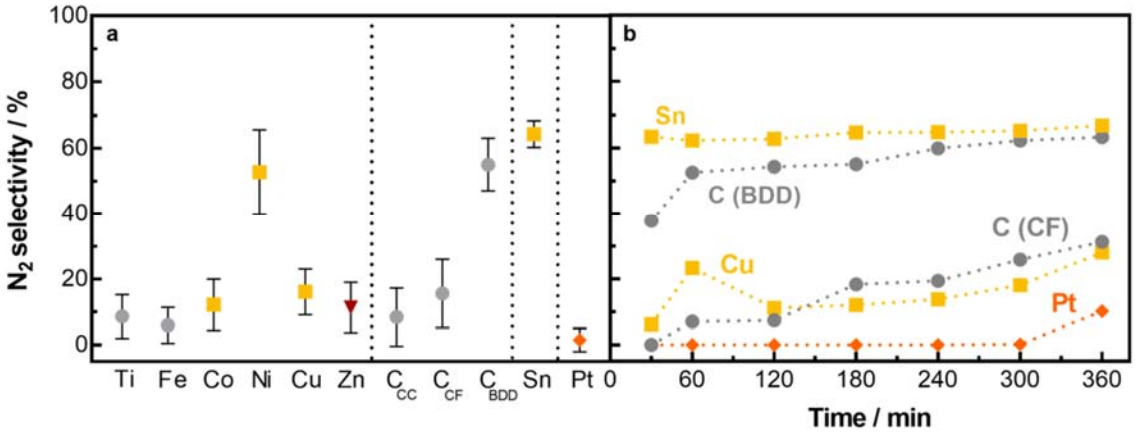

Figure 5. (a) Average and standard deviation of the selectivity towards N_2 obtained with the different cathodic materials studied during the ERN treatment. (b) Selectivity towards N_2 over time for selected electrodes. Note: CC, CF, and BDD stands for carbon cloth, carbon felt, and boron-doped diamond, respectively. Conditions: 100 mg L^{-1} NO_3^--N in 50 mM Na_2SO_4 at 20 mA cm^{-2}. Elements availability: (●) high abundance, (■) limited availability, (◆) rising threat, (▼) serious threat in next 100 years.

Effective electrocatalysts should have the attributes of rapid nitrate removal (i.e., high k_1) with a corresponding high selectivity towards desired N-gas by-products (i.e., high $S_{N_{gas}}$). For electrode materials illustrated in Figure 4, the more effective materials are located in the upper-right quadrant. Thus, Sn and carbon-based BDD would be classified as the most effective for nitrate

333 removal and are clearly superior to commercial polycrystalline Pt electrodes, which achieved only
334 1% selectivity towards N-gases.

335 Other material factors can impact electrocatalyst effectiveness for use in drinking water.
336 Most notably, corrosion of some electrodes may impart regulatory concerns or long-term
337 operability challenges. Among the metals investigated, only Cu is included in primary drinking
338 water regulations, where levels above 0.8 mg L^{-1} begin to pose health concerns. Such high levels
339 would be detrimental to the electrode itself and would therefore need to be studied in more detail.
340 Fe and Zn have similarly high secondary drinking water limits, set by aesthetics rather than health
341 limits, of 0.3 and 5 mg L^{-1}, respectively. Other metals (Ti, Co, Ni, Sn) are not regulated in drinking
342 water. While carbon is not directly regulated, numerous organic carbon compounds (e.g.,
343 polyaromatic hydrocarbons) are regulated as carcinogens, but their evolution from graphitic or
344 diamond forms of carbon are unlikely. Thus, considering drinking water contaminant limits
345 wouldn't change the above recommendation to focus on BDD- or Sn-based electrodes.
346

347 **3.4 Energy-based figures of merit considerations**

348 Beyond performance (i.e., nitrate removal rates and by-product formation), energy
349 efficiency will also contribute to electrode element selection. Electrochemical reduction
350 effectiveness is commonly evaluated in terms of Faradaic efficiency (FE, Eq. (3)) for N_2 evolution.
351 Figure 6a shows FE over time for selected electrocatalysts and demonstrates competitive
352 alternatives to conventional Pt electrodes in terms of superior kinetics and selectivity.
353 Electrocatalysts with low selectivity for N_2 (i.e., Pt, Cu, carbon felt) accordingly had low FE,
354 ranging between 0% and 7%. Meanwhile, promising BDD and Sn electrodes had FEs between 10
355 and 22%. Both BDD and Sn showed an analogous decrease in FE over electrolysis time. This
356 behavior can be related to the nitrate concentration decrease over time, whereas the electric current
357 is the same. Consequently, the kinetics of parasitic reactions, such as hydrogen evolution, may be
358 enhanced[72,74], resulting in a lower final FE.

Engineering figures of merit provide a different, practical method to assess process energy efficiency across multiple options. Because the WHO recommends ~11 mg L^{-1} as NO_3^--N and our experiments had initial nitrate concentrations of 100 mg NO_3^--N, the E_{EO} is shown for one order of magnitude decrease in nitrate (kWh m^{-3} $order^{-1}$, Figure 6b). Under identical electrochemical cell reactor configurations, E_{EO} ranged between 30 and 50 kWh m^{-3} $order^{-1}$. For the two most effective materials from Figure 4 (i.e., Sn and BDD), E_{EO} was 39 and 49 kWh m^{-3} $order^{-1}$, respectively. E_{EO} at a given applied current is controlled by two main factors: (a) nitrate reduction rate k_1 and (b) the cell potential (E_{cell}). Although Sn and BDD had a comparable kinetic constant for nitrate removal, the cell potential average (E_{cell}) for each is different. The E_{cell} was 5.4 V for Sn and 7.0 V for BDD, which resulted in a higher E_{EO} for the BDD cathode. The interdependence between k_1 and E_{cell} explain why the E_{EO} for Pt (47 kWh m^{-3} $order^{-1}$) is between the ones for Sn and BDD. Other research shows that E_{EO} can be decreased by >10-fold from the observed values through engineering design of electrode morphology, electrode spacing, and hydrodynamics[22,23,73]. For example, flow-through electrodes are superior to flow-by electrodes because the former exhibits lower mass transfer limitations for target pollutants/by-products towards/from the electrode surface. Fortunately, many of the elements, including BDD and Sn, can be engineered into almost any integrated electrode and reactor configuration.

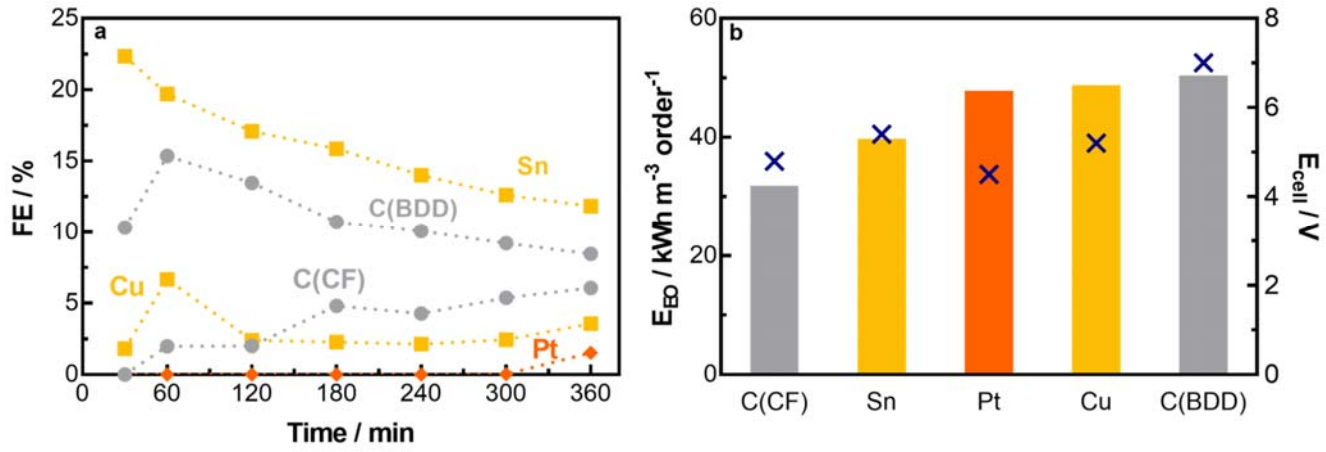

Figure 6. (a) Faradaic efficiency (FE) over time, (b) energy consumption per order (bars) and cell potential average (×) for the electroreduction of 100 mg L^{-1} NO_3^--N in 50 mM Na_2SO_4 at 20 mA cm^{-2}, using Cu, C-CF, C-BDD, Sn, and Pt as cathode materials. Note: CF and BDD stand for carbon felt and boron-doped diamond, respectively. Elements availability: (●) high abundance, (■) limited availability, (◆) rising threat, (▼) serious threat in next 100 years.

4. Conclusions

This work applies a framework for screening earth-abundant electrode materials under identical operating conditions to obtain figures of merit suitable to identify more sustainable electrocatalytic systems that can remove nitrate from drinking waters. Platinum (Pt), a well-studied electrocatyst in the literature, was selected as a benchmark electrode representing the PGEs. Electrokinetic pseudo first-order nitrate degradation rates (k_1) were slightly better (~50% larger k_1) for Cu-, C-, and Sn-based electrodes relative to Pt. The difference in selectivity towards the preferential by-products (i.e., N-gases) showed tremendous promise for more earth-abundant elements, being up to 7-fold more selective ($S_{N_{gas}}$ of 55% and 64% for BDD and Sn, respectively) than the PGE-based electrode ($S_{N_{gas}}$~1% for Pt). Degradation rates and selectivities impacted Faradaic efficiency and E_{EO}. No adverse effects were shown on these figures of merit when transitioning electrode material from PGE to more sustainable elements (e.g., Sn, BDD).

Each element used in the electrodes has a commodity market cost ($ kg^{-1}). The structure of catalytic materials, with crystallites of different sizes and orientations, are critical to maximize the selectivity towards the preferred by-product species (N_2 gas). Electrode manufacturing to transform the base element into the plethora of electrode architectures (e.g., high porosity electrodes) will add to the cost of the final electrode. For example, while carbon is the cheapest commodity element, the three carbon-based electrodes showed that different morphologies, oxidation states, and crystallites can lead to very different reaction outcomes. Thus, while acknowledging it may be premature to

draw a specific selection of electrodes in terms of performance-cost analysis, this work provides an initial roadmap on expected cost depending on the element source. A complete techno-economic analysis will be conducted in a well-developed electrocatalytic system considering electrode life and its manufacturing associated costs.

The above framework identified the application of earth-abundant materials, which global availability is not endangered, to electrochemical nitrate reduction. This represents a game changer for developing low-cost electrocatalytic-based treatment water systems, where Pt-based catalysts have been shown to be cost prohibitive (e.g., [40,41]). Sn-based and carbonaceous electrodes (i.e., BDD) were recognized as viable earth-abundant electrocatalysts alternatives to endangered elements. Innovations in electrode manufacturing are still needed to reduce capital costs and E_{EO} by optimizing mass transport. This may occur by maximizing surface area of the more reactive and stable surfaces of earth-abundant elements as electrodes. Future research using nanotechnology with earth-abundant materials can exploit opportunities[75], enabling catalytic sites that specifically tailor nitrate reduction towards innocuous nitrogen gas, further increasing the competitiveness of POU systems.

Acknowledgments

This project has received funding from the European Union's Horizon 2020 research and innovation program under the Marie Sklodowska-Curie grant agreement No 843870. This work was partially funded by the National Science Foundation (NSF) through the Nanotechnology-Enabled Water Treatment Nanosystems Engineering Research Center under project EEC-1449500. Laurel Passantino provided technical editing.

References

[1] UN, UN Sustainable Development Goals, 2018. https://sustainabledevelopment.un.org/?menu=1300.

[2] EPA, Estimated nitrate concentrations in groundwater used for drinking, 2017. https://www.epa.gov/nutrient-policy-data/estimated-nitrate-concentrations-groundwater-used-drinking.

[3] Y. Zhai, Y. Lei, J. Wu, Y. Teng, J. Wang, X. Zhao, X. Pan, Does the groundwater nitrate pollution in China pose a risk to human health? A critical review of published data, Environ. Sci. Pollut. Res. 24 (2017) 3640–3653. https://doi.org/10.1007/s11356-016-8088-9.

[4] M. Allaire, H. Wu, U. Lall, National trends in drinking water quality violations, Proc. Natl. Acad. Sci. U. S. A. 115 (2018) 2078–2083. https://doi.org/10.1073/pnas.1719805115.

[5] D. Han, M.J. Currell, G. Cao, Deep challenges for China's war on water pollution, Environ. Pollut. 218 (2016) 1222–1233. https://doi.org/10.1016/j.envpol.2016.08.078.

[6] WHO, Nitrate and nitrite in drinking-water, 2016. https://www.who.int/water_sanitation_health/dwq/chemicals/nitrate-nitrite-background-jan17.pdf?ua=1.

[7] EPA, National primary drinking water regulations, 2017. https://www.epa.gov/ground-water-and-drinking-water/national-primary-drinking-water-regulations.

[8] R.R. Jones, P.J. Weyer, C.T. Dellavalle, M. Inoue-Choi, K.E. Anderson, K.P. Cantor, S. Krasner, K. Robien, L.E. Beane Freeman, D.T. Silverman, M.H. Ward, Nitrate from drinking water and diet and bladder cancer among postmenopausal women in Iowa, Environ. Health Perspect. 124 (2016) 1751–1758. https://doi.org/10.1289/EHP191.

[9] A. Temkin, S. Evans, T. Manidis, C. Campbell, O. V. Naidenko, Exposure-based assessment and economic valuation of adverse birth outcomes and cancer risk due to nitrate in United States drinking water., Environ. Res. 176 (2019) 108442. https://doi.org/10.1016/j.envres.2019.04.009.

[10] J. Schullehner, B. Hansen, M. Thygesen, C.B. Pedersen, T. Sigsgaard, Nitrate in drinking water and colorectal cancer risk: A nationwide population-based cohort study, Int. J. Cancer. 143 (2018) 73–79. https://doi.org/10.1002/ijc.31306.

[11] A.H. Wolfe, J.A. Patz, Reactive nitrogen and human health: Acute and long-term implications, Ambio. 31 (2002) 120–125. https://doi.org/10.1579/0044-7447-31.2.120.

[12] M.H. Ward, R.R. Jones, J.D. Brender, T.M. de Kok, P.J. Weyer, B.T. Nolan, C.M. Villanueva, S.G. van Breda, Drinking water nitrate and human health: An updated review, Int. J. Environ. Res. Public Health. 15 (2018) 1–31. https://doi.org/10.3390/ijerph15071557.

[13] M.J. Pennino, J.E. Compton, S.G. Leibowitz, Trends in Drinking Water Nitrate Violations Across the United States, Environ. Sci. Technol. 51 (2017) 13450–13460. https://doi.org/10.1021/acs.est.7b04269.

[14] Y. Ren, Y. Ye, J. Zhu, K. Hu, Y. Wang, Characterization and evaluation of a macroporous anion exchange resin for nitrate removal from drinking water, Desalin. Water Treat. 57 (2016) 17430–17439. https://doi.org/10.1080/19443994.2015.1085450.

[15] EPA, Nitrate removal from water supplies by ion exchange, 1978. https://nepis.epa.gov/Exe/ZyNET.exe/9102065Y.TXT?ZyActionD=ZyDocument&Client=EPA&Index=1976+Thru+1980&Docs=&Query=&Time=&EndTime=&SearchMethod=1&TocRestrict=n&Toc=&TocEntry=&QField=&QFieldYear=&QFieldMonth=&QFieldDay=&IntQFieldOp=0&ExtQFieldOp=0&XmlQuery=.

[16] A. Breytus, D. Hasson, R. Semiat, H. Shemer, Removal of nitrate from groundwater by Donnan dialysis, J. Water Process Eng. 34 (2020) 101157. https://doi.org/10.1016/j.jwpe.2020.101157.

[17] J.W. Palko, D.I. Oyarzun, B. Ha, M. Stadermann, J.G. Santiago, Nitrate removal from water using electrostatic regeneration of functionalized adsorbent, Chem. Eng. J. 334 (2018) 1289–1296. https://doi.org/10.1016/j.cej.2017.10.161.

[18] Q. Li, X. Lu, C. Shuang, C. Qi, G. Wang, A. Li, H. Song, Preferential adsorption of nitrate with different trialkylamine modified resins and their preliminary investigation for advanced treatment of municipal wastewater, Chemosphere. 223 (2019) 39–47. https://doi.org/10.1016/j.chemosphere.2019.02.008.

[19] V.B. Jensen, J.L. Darby, C. Seidel, C. Gorman, Nitrate in potable water supplies: Alternative management strategies, Crit. Rev. Environ. Sci. Technol. 44 (2014) 2203–2286. https://doi.org/10.1080/10643389.2013.828272.

[20] S. Garcia-Segura, A.B. Nienhauser, A.S. Fajardo, R. Bansal, C.L. Coonrod, J.D. Fortner, M. Marcos-Hernández, T. Rogers, D. Villagran, M.S. Wong, P. Westerhoff, Disparities between experimental and environmental conditions: Research steps toward making electrochemical water treatment a reality, Curr. Opin. Electrochem. 22 (2020) 9–16. https://doi.org/10.1016/j.coelec.2020.03.001.

[21] L. Liu, E. Lopez, L. Dueñas-Osorio, L. Stadler, Y. Xie, P.J.J. Alvarez, Q. Li, The importance of system configuration for distributed direct potable water reuse, Nat. Sustain. (2020). https://doi.org/10.1038/s41893-020-0518-5.

[22] S. Garcia-Segura, M. Lanzarini-Lopes, K. Hristovski, P. Westerhoff, Electrocatalytic reduction of nitrate: Fundamentals to full-scale water treatment applications, Appl. Catal. B Environ. 236 (2018) 546–568. https://doi.org/10.1016/j.apcatb.2018.05.041.

[23] B.P. Chaplin, The Prospect of Electrochemical Technologies Advancing Worldwide Water Treatment, Acc. Chem. Res. 52 (2019) 596–604. https://doi.org/10.1021/acs.accounts.8b00611.

[24] R. Stirling, W.S. Walker, P. Westerhoff, S. Garcia-Segura, Techno-economic analysis to identify key innovations required for electrochemical oxidation as point-of-use treatment systems, Electrochim. Acta. 338 (2020) 135874. https://doi.org/10.1016/j.electacta.2020.135874.

[25] K. Nishimura, K. Machida, M. Enyo, On-line mass spectroscopy applied to electroreduction of nitrite and nitrate ions at porous Pt electrode in sulfuric acid solutions, Electrochim. Acta. 36 (1991) 877–880. https://doi.org/10.1016/0013-4686(91)85288-I.

[26] J.F.E. Gootzen, P.G.J.M. Peeters, J.M.B. Dukers, L. Lefferts, W. Visscher, J.A.R. Van Veen, The electrocatalytic reduction of NO-3 on Pt, Pd and Pt + Pd electrodes activated with Ge, J.

507 Electroanal. Chem. 434 (1997) 171–183. https://doi.org/10.1016/S0022-0728(97)00093-4.
508 [27] S. Ureta-Zañartu, C. Yáñez, Electroreduction of nitrate ion on Pt, Ir and on 70:30 Pt:Ir alloy,
509 Electrochim. Acta. 42 (1997) 1725–1731. https://doi.org/10.1016/S0013-4686(96)00372-6.
510 [28] G.E. Dima, A.C.A. De Vooys, M.T.M. Koper, Electrocatalytic reduction of nitrate at low
511 concentration on coinage and transition-metal electrodes in acid solutions, J. Electroanal.
512 Chem. 554–555 (2003) 15–23. https://doi.org/10.1016/S0022-0728(02)01443-2.
513 [29] M.T. De Groot, M.T.M. Koper, The influence of nitrate concentration and acidity on the
514 electrocatalytic reduction of nitrate on platinum, J. Electroanal. Chem. 562 (2004) 81–94.
515 https://doi.org/10.1016/j.jelechem.2003.08.011.
516 [30] G.E. Dima, G.L. Beltramo, M.T.M. Koper, Nitrate reduction on single-crystal platinum
517 electrodes, Electrochim. Acta. 50 (2005) 4318–4326.
518 https://doi.org/10.1016/j.electacta.2005.02.093.
519 [31] E. Lacasa, P. Cañizares, J. Llanos, M.A. Rodrigo, Effect of the cathode material on the
520 removal of nitrates by electrolysis in non-chloride media, J. Hazard. Mater. 213–214 (2012)
521 478–484. https://doi.org/10.1016/j.jhazmat.2012.02.034.
522 [32] K.N. Heck, S. Garcia-Segura, P. Westerhoff, M.S. Wong, Catalytic Converters for Water
523 Treatment, Acc. Chem. Res. 52 (2019) 906–915.
524 https://doi.org/10.1021/acs.accounts.8b00642.
525 [33] M.M. Hossain, T. Kawaguchi, K. Shimazu, K. Nakata, Reduction of nitrate on tin-modified
526 palladium-platinum electrodes, J. Electroanal. Chem. 864 (2020) 114041.
527 https://doi.org/10.1016/j.jelechem.2020.114041.
528 [34] Y.J. Shih, Z.L. Wu, C.Y. Lin, Y.H. Huang, C.P. Huang, Manipulating the crystalline
529 morphology and facet orientation of copper and copper-palladium nanocatalysts supported
530 on stainless steel mesh with the aid of cationic surfactant to improve the electrochemical
531 reduction of nitrate and N2 selectivity, Appl. Catal. B Environ. 273 (2020) 119053.
532 https://doi.org/10.1016/j.apcatb.2020.119053.

[35] M. Cao, D. Wu, R. Cao, Recent advances in the stabilization of platinum electrocatalysts for fuel-cell reactions, ChemCatChem. 6 (2014) 26–45. https://doi.org/10.1002/cctc.201300647.

[36] C.M. Sánchez-Sánchez, J. Souza-Garcia, E. Herrero, A. Aldaz, Electrocatalytic reduction of carbon dioxide on platinum single crystal electrodes modified with adsorbed adatoms, J. Electroanal. Chem. 668 (2012) 51–59. https://doi.org/10.1016/j.jelechem.2011.11.002.

[37] P.B. Kettler, Platinum group metals in catalysis: Fabrication of catalysts and catalyst precursors, Org. Process Res. Dev. 7 (2003) 342–354. https://doi.org/10.1021/op034017o.

[38] ACS, Endangered elements, 2019. https://www.acs.org/content/acs/en/greenchemistry/research-innovation/endangered-elements.html.

[39] P. Chirik, R. Morris, Getting Down to Earth: The Renaissance of Catalysis with Abundant Metals, Acc. Chem. Res. 48 (2015) 2495. https://doi.org/10.1021/acs.accounts.5b00385.

[40] J.K. Choe, A.M. Bergquist, S. Jeong, J.S. Guest, C.J. Werth, T.J. Strathmann, Performance and life cycle environmental benefits of recycling spent ion exchange brines by catalytic treatment of nitrate, Water Res. 80 (2015) 267–280. https://doi.org/10.1016/j.watres.2015.05.007.

[41] X. Chen, X. Huo, J. Liu, Y. Wang, C.J. Werth, T.J. Strathmann, Exploring beyond palladium: Catalytic reduction of aqueous oxyanion pollutants with alternative platinum group metals and new mechanistic implications, Chem. Eng. J. 313 (2017) 745–752. https://doi.org/10.1016/j.cej.2016.12.058.

[42] É. Lèbre, J.R. Owen, G.D. Corder, D. Kemp, M. Stringer, R.K. Valenta, Source Risks As Constraints to Future Metal Supply, Environ. Sci. Technol. 53 (2019) 10571–10579. https://doi.org/10.1021/acs.est.9b02808.

[43] EPA, Method 300.0 - Determination of inorganic anions by Ion Chromatography, 1993. https://www.epa.gov/sites/production/files/2015-08/documents/method_300-0_rev_2-1_1993.pdf.

559 [44] I. Sanjuán, L. García-Cruz, J. Solla-Gullón, E. Expósito, V. Montiel, Bi–Sn nanoparticles for
560 electrochemical denitrification: activity and selectivity towards N2 formation, Electrochim.
561 Acta. 340 (2020). https://doi.org/10.1016/j.electacta.2020.135914.
562 [45] D. Yin, Y. Liu, P. Song, P. Chen, X. Liu, L. Cai, L. Zhang, In situ growth of copper/reduced
563 graphene oxide on graphite surfaces for the electrocatalytic reduction of nitrate, Electrochim.
564 Acta. 324 (2019) 134846. https://doi.org/10.1016/j.electacta.2019.134846.
565 [46] M. Lanzarini-Lopes, S. Garcia-Segura, K. Hristovski, P. Westerhoff, Electrical energy per
566 order and current efficiency for electrochemical oxidation of p-chlorobenzoic acid with
567 boron-doped diamond anode, Chemosphere. 188 (2017) 304–311.
568 https://doi.org/10.1016/j.chemosphere.2017.08.145.
569 [47] E.B. Molodkina, M.R. Ehrenburg, Y.M. Polukarov, A.I. Danilov, J. Souza-Garcia, J.M.
570 Feliu, Electroreduction of nitrate ions on Pt(1 1 1) electrodes modified by copper adatoms,
571 Electrochim. Acta. 56 (2010) 154–165. https://doi.org/10.1016/j.electacta.2010.08.105.
572 [48] M.C. Figueiredo, J. Solla-Gullón, F.J. Vidal-Iglesias, V. Climent, J.M. Feliu, Nitrate
573 reduction at Pt(1 0 0) single crystals and preferentially oriented nanoparticles in neutral
574 media, Catal. Today. 202 (2013) 2–11. https://doi.org/10.1016/j.cattod.2012.02.038.
575 [49] S. Taguchi, J.M. Feliu, Electrochemical reduction of nitrate on Pt(S)[n(1 1 1) × (1 1 1)]
576 electrodes in perchloric acid solution, Electrochim. Acta. 52 (2007) 6023–6033.
577 https://doi.org/10.1016/j.electacta.2007.03.057.
578 [50] S. Amertharaj, M.A. Hasnat, N. Mohamed, Electroreduction of nitrate ions at a platinum-
579 copper electrode in an alkaline medium: Influence of sodium inositol phytate, Electrochim.
580 Acta. 136 (2014) 557–564. https://doi.org/10.1016/j.electacta.2014.05.128.
581 [51] J. Yang, M. Duca, K.J.P. Schouten, M.T.M. Koper, Formation of volatile products during
582 nitrate reduction on a Sn-modified Pt electrode in acid solution, J. Electroanal. Chem. 662
583 (2011) 87–92. https://doi.org/10.1016/j.jelechem.2011.03.015.
584 [52] K.-W. Kim, S.-M. Kim, Y.-H. Kim, E.-H. Lee, K.-Y. Jee, Sn Stability of Sn-Modified Pt

585 Electrode for Reduction of Nitrate, J. Electrochem. Soc. 154 (2007) E145.
586 https://doi.org/10.1149/1.2769286.
587 [53] J. Martínez, A. Ortiz, I. Ortiz, State-of-the-art and perspectives of the catalytic and
588 electrocatalytic reduction of aqueous nitrates, Appl. Catal. B Environ. 207 (2017) 42–59.
589 https://doi.org/10.1016/j.apcatb.2017.02.016.
590 [54] M. Duca, N. Sacré, A. Wang, S. Garbarino, D. Guay, Enhanced electrocatalytic nitrate
591 reduction by preferentially-oriented (100) PtRh and PtIr alloys: the hidden treasures of the
592 'miscibility gap,' Appl. Catal. B Environ. 221 (2018) 86–96.
593 https://doi.org/10.1016/j.apcatb.2017.08.081.
594 [55] X. Ma, M. Li, C. Feng, W. Hu, L. Wang, X. Liu, Development and reaction mechanism of
595 efficient nano titanium electrode: Reconstructed nanostructure and enhanced nitrate removal
596 efficiency, J. Electroanal. Chem. 782 (2016) 270–277.
597 https://doi.org/10.1016/j.jelechem.2016.10.047.
598 [56] W. Li, C. Xiao, Y. Zhao, Q. Zhao, R. Fan, J. Xue, Electrochemical Reduction of High-
599 Concentrated Nitrate Using Ti/TiO2 Nanotube Array Anode and Fe Cathode in Dual-
600 Chamber Cell, Catal. Letters. 146 (2016) 2585–2595. https://doi.org/10.1007/s10562-016-
601 1894-3.
602 [57] V.K. Sharma, Oxidation of nitrogen-containing pollutants by novel ferrate(VI) technology:
603 A review, J. Environ. Sci. Heal. - Part A Toxic/Hazardous Subst. Environ. Eng. 45 (2010)
604 645–667. https://doi.org/10.1080/10934521003648784.
605 [58] M.C.P.M. Da Cunha, J.P.I. De Souza, F.C. Nart, Reaction pathways for reduction of nitrate
606 ions on platinum, rhodium, and platinum-rhodium alloy electrodes, Langmuir. 16 (2000)
607 771–777. https://doi.org/10.1021/la990638s.
608 [59] M. Duca, M.T.M. Koper, Powering denitrification: The perspectives of electrocatalytic
609 nitrate reduction, Energy Environ. Sci. 5 (2012) 9726–9742.
610 https://doi.org/10.1039/c2ee23062c.

611 [60] M. Duca, M.O. Cucarella, P. Rodriguez, M.T.M. Koper, Direct reduction of nitrite to N2 on
612 a Pt(100) electrode in alkaline media, J. Am. Chem. Soc. 132 (2010) 18042–18044.
613 https://doi.org/10.1021/ja1092503.
614 [61] T. Chen, H. Li, H. Ma, M.T.M. Koper, Surface Modification of Pt(100) for Electrocatalytic
615 Nitrate Reduction to Dinitrogen in Alkaline Solution, Langmuir. 31 (2015) 3277–3281.
616 https://doi.org/10.1021/acs.langmuir.5b00283.
617 [62] M. Duca, M.C. Figueiredo, V. Climent, P. Rodriguez, J.M. Feliu, M.T.M. Koper, Selective
618 catalytic reduction at quasi-perfect Pt(100) domains: A universal low-temperature pathway
619 from nitrite to N2, J. Am. Chem. Soc. 133 (2011) 10928–10939.
620 https://doi.org/10.1021/ja203234v.
621 [63] M.C.P.M. Da Cunha, M. Weber, F.C. Nart, On the adsorption and reduction of NO3- ions at
622 Au and Pt electrodes studied by in situ FTIR spectroscopy, J. Electroanal. Chem. 414 (1996)
623 163–170. https://doi.org/10.1016/0022-0728(96)04697-9.
624 [64] J.M. McEnaney, S.J. Blair, A.C. Nielander, J.A. Schwalbe, D.M. Koshy, M. Cargnello, T.F.
625 Jaramillo, Electrolyte engineering for efficient electrochemical nitrate reduction to ammonia
626 on a titanium electrode, ACS Sustain. Chem. Eng. 8 (2020) 2672–2681.
627 https://doi.org/10.1021/acssuschemeng.9b05983.
628 [65] L. Rajic, D. Berroa, S. Gregor, S. Elbakri, M. MacNeil, A.N. Alshawabkeh,
629 Electrochemically-induced reduction of nitrate in aqueous solution, Int. J. Electrochem. Sci.
630 12 (2017) 5998–6009. https://doi.org/10.20964/2017.07.38.
631 [66] F. Yao, Q. Yang, Y. Zhong, X. Shu, F. Chen, J. Sun, Y. Ma, Z. Fu, D. Wang, X. Li, Indirect
632 electrochemical reduction of nitrate in water using zero-valent titanium anode: Factors,
633 kinetics, and mechanism, Water Res. 157 (2019) 191–200.
634 https://doi.org/10.1016/j.watres.2019.03.078.
635 [67] J. Lai, A. Nsabimana, R. Luque, G. Xu, 3D Porous Carbonaceous Electrodes for
636 Electrocatalytic Applications, Joule. 2 (2018) 76–93.

637 https://doi.org/10.1016/j.joule.2017.10.005.
638 [68] J. Ding, W. Li, Q.L. Zhao, K. Wang, Z. Zheng, Y.Z. Gao, Electroreduction of nitrate in
639 water: Role of cathode and cell configuration, Chem. Eng. J. 271 (2015) 252–259.
640 https://doi.org/10.1016/j.cej.2015.03.001.
641 [69] K. Naga Mahesh, R. Balaji, K.S. Dhathathreyan, Studies on noble metal-free carbon-based
642 cathodes for magnesium–hydrogen peroxide fuel cells, Ionics (Kiel). 21 (2015) 2603–2607.
643 https://doi.org/10.1007/s11581-015-1434-y.
644 [70] W. Chen, D. Wu, H. Wan, R. Tang, C. Li, G. Wang, C. Feng, Carbon-based cathode as an
645 electron donor driving direct bioelectrochemical denitrification in biofilm-electrode reactors:
646 Role of oxygen functional groups, Carbon N. Y. 118 (2017) 310–318.
647 https://doi.org/10.1016/j.carbon.2017.03.062.
648 [71] M. Villanueva-Rodríguez, C.M. Sánchez-Sánchez, V. Montiel, E. Brillas, J.M. Peralta-
649 Hernández, A. Hernández-Ramírez, Characterization of ferrate ion electrogeneration in
650 acidic media by voltammetry and scanning electrochemical microscopy. Assessment of its
651 reactivity on 2,4-dichlorophenoxyacetic acid degradation, Electrochim. Acta. 64 (2012)
652 196–204. https://doi.org/10.1016/j.electacta.2012.01.021.
653 [72] P. Kuang, K. Natsui, Y. Einaga, Comparison of performance between boron-doped diamond
654 and copper electrodes for selective nitrogen gas formation by the electrochemical reduction
655 of nitrate, Chemosphere. 210 (2018) 524–530.
656 https://doi.org/10.1016/j.chemosphere.2018.07.039.
657 [73] L. Guo, Y. Jing, B.P. Chaplin, Development and Characterization of Ultrafiltration TiO2
658 Magnéli Phase Reactive Electrochemical Membranes, Environ. Sci. Technol. 50 (2016)
659 1428–1436. https://doi.org/10.1021/acs.est.5b04366.
660 [74] I. Katsounaros, D. Ipsakis, C. Polatides, G. Kyriacou, Efficient electrochemical reduction of
661 nitrate to nitrogen on tin cathode at very high cathodic potentials, Electrochim. Acta. 52
662 (2006) 1329–1338. https://doi.org/10.1016/j.electacta.2006.07.034.

663 [75] M.S. Mauter, I. Zucker, F. Perreault, J.R. Werber, J.H. Kim, M. Elimelech, The role of
664 nanotechnology in tackling global water challenges, Nat. Sustain. 1 (2018) 166–175.
665 https://doi.org/10.1038/s41893-018-0046-8.
666